cancers

MDPI

Article

Al[^{18}F]F-NOTA-Octreotide Is Comparable to [^{68}Ga]Ga-DOTA-TATE for PET/CT Imaging of Neuroendocrine Tumours in the Latin-American Population

Arlette Haeger [1,*,†], Cristian Soza-Ried [1,2,†], Vasko Kramer [1,2], Ana Hurtado de Mendoza [1], Elisabeth Eppard [1,3], Noémie Emmanuel [4], Johanna Wettlin [1], Horacio Amaral [1,2] and René Fernández [1]

1 Nuclear Medicine and PET/CT Center PositronMed, Providencia, Santiago 7501068, Chile
2 Positronpharma SA, Providencia, Santiago 7500921, Chile
3 Department of Nuclear Medicine, University Hospital Magdeburg, 39120 Magdeburg, Germany
4 Ion Beam Applications, 1348 Louvain-la-Neuve, Belgium
* Correspondence: ahaeger@positronmed.cl
† These authors contributed equally to this work.

Simple Summary: In the present work we investigated the clinical utility of Al[^{18}F]F-NOTA-Octreotide (Al[^{18}F]F-OC) in comparison to [^{68}Ga]Ga-DOTA-TATE in patients diagnosed with neuroendocrine tumours. Our aim was to verify the recently published, promising results for Al[^{18}F]F-NOTA-Octreotide in the Latin-American population. Al[^{18}F]F-NOTA-Octreotide provided excellent image quality, detected NET lesions with high sensitivity and represents a highly promising, clinical alternative to [^{68}Ga]Ga-DOTA-TATE.

Abstract: PET imaging of neuroendocrine tumours (NET) is well established for staging and therapy follow-up. The short half-life, increasing costs, and regulatory issues significantly limit the availability of approved imaging agents, such as [^{68}Ga]Ga-DOTA-TATE. Al[^{18}F]F-NOTA-Octreotide provides a similar biodistribution and tumour uptake, can be produced on a large scale and may improve access to precision imaging. Here we prospectively compared the clinical utility of [^{68}Ga]Ga-DOTA-TATE and Al[^{18}F]F-NOTA-Octreotide in the Latin-American population. Our results showed that in patients with stage IV NETs [^{68}Ga]Ga-DOTA-TATE presents higher physiological uptake than Al[^{18}F]F-NOTA-Octreotide in the liver, hypophysis, salivary glands, adrenal glands (all $p < 0.001$), pancreatic uncinated process, kidneys, and small intestine (all $p < 0.05$). Nevertheless, despite the lower background uptake of Al[^{18}F]F-NOTA-Octreotide, comparative analysis of tumour-to-liver (TLR) and tumour-to-spleen (TSR) showed no statistically significant difference for lesions in the liver, bone, lymph nodes, and other tissues. Only three discordant lesions in highly-metastases livers were detected by [^{68}Ga]Ga-DOTA-TATE but not by Al[^{18}F]F-NOTA-Octreotide and only one discordant lesion was detected by Al[^{18}F]F-NOTA-Octreotide but not by [^{68}Ga]Ga-DOTA-TATE. Non-inferiority analysis showed that Al[^{18}F]F-NOTA-Octreotide is comparable to [^{68}Ga]Ga-DOTA-TATE. Hence, our results demonstrate that Al[^{18}F]F-NOTA-Octreotide provided excellent image quality, visualized NET lesions with high sensitivity and represents a highly promising, clinical alternative to [^{68}Ga]Ga-DOTA-TATE.

Keywords: neuroendocrine tumours; SSTR; Al[^{18}F]F-NOTA-Octreotide; PET imaging

Citation: Haeger, A.; Soza-Ried, C.; Kramer, V.; Hurtado de Mendoza, A.; Eppard, E.; Emmanuel, N.; Wettlin, J.; Amaral, H.; Fernández, R. Al[^{18}F]F-NOTA-Octreotide Is Comparable to [^{68}Ga]Ga-DOTA-TATE for PET/CT Imaging of Neuroendocrine Tumours in the Latin-American Population. *Cancers* **2023**, *15*, 439. https://doi.org/10.3390/cancers15020439

Academic Editor: Tsuyoshi Sugiura

Received: 14 December 2022
Revised: 4 January 2023
Accepted: 5 January 2023
Published: 10 January 2023

1. Introduction

Neuroendocrine tumours (NETs) are highly heterogeneous neoplasms that arise from neuroendocrine cells and affect the diffuse neuroendocrine system, intestinal tract and bronchia [1]. The slow progression of these tumours and their unspecific symptoms lead to a high prevalence and late diagnoses [2–4]. Unfortunately, late diagnoses favour the development of distant metastasis resulting in high mortality [5]. To improve the clinical

outcome for NET patients, early detection of these tumours before dissemination is of utmost importance. NETs are characterised by the high expression of somatostatin receptors (SSTR) [6], chromogranin A and synaptophysin [7]. SSTR is a G protein-coupled receptor that binds the somatostatin neuropeptide, which is paracrine secreted by gastrointestinal and brain cells. Although there are five SSTR subtypes (SSTR 1–5), 80% of NETs overexpress SSTR2 [8]. Diagnostic imaging, staging, and follow-up after treatment can be performed by single-photon emission computed tomography (SPECT/CT) or positron emission tomography/computed tomography (PET/CT) with radiolabelled somatostatin analogues [9]. To this end, radiotracers such as [^{68}Ga]Ga-DOTA-TATE, [^{68}Ga]Ga-DOTA-TOC, and [^{68}Ga]Ga-DOTA-NOC are the standard radiopharmaceuticals for NET detection [10–12]. PET imaging of SSTR is further required for pretherapeutic evaluation of patients who are candidates for SSTR-targeted therapy with [^{177}Lu]Lu-DOTA-TATE [13].

However, the high cost of ^{68}Ge/^{68}Ga generators [9], the short half-life of Galium-68 (68 min), regulatory and quality assurance aspects significantly limit the availability of these tracers, especially in Latin-America and developing countries. Fluorine-18 has a longer half-life (109.8 min) and a better spatial resolution as compared to Gallium-68 due to the lower positron-energy [9,14,15]. Several ^{18}F-labelled SSTR-radioligands have been developed in recent years which can be produced in large scale and satellite-distribution over longer distances is feasible [16]. Al[^{18}F]F-NOTA-Octreotide is one of the most promising candidates [14,15,17,18], providing a high affinity for SSTR2 [17,19], a favourable biodistribution, high tumour uptake and has proven to be safe in clinical applications [15].

Several studies have compared Al[^{18}F]F-NOTA-Octreotide and [^{68}Ga]Ga-DOTA-TATE PET imaging in NET patients showing outstanding results [14,20–22]. A first comparison was published in a case report by Pauwels et al. in 2019 and, despite their different chemical structures (Figure S1), both ligands showed a very similar biodistribution in healthy organs and NET lesions [20]. These initial results were confirmed in a systematic evaluation of six NET patients by the same group[21] and independently in a study conducted by Hou et al. including 20 NET patients [14]. Both studies proofed the non-inferiority of Al[^{18}F]F-NOTA-Octreotide and showed even higher tumour-to-liver ratios (TLR) as compared to [^{68}Ga]Ga-DOTA-TATE [14,21]. Finally, a recent, prospective study in 75 patients found that Al[^{18}F]F-NOTA-Octreotide outperformed [^{68}Ga]Ga-DOTA-TATE showing significantly higher detection rates and tumour-to-background ratios when PET images were acquired two hours post injection [22]. Given the limited access to [^{68}Ga]Ga-DOTA-TATE in vast countries, such as Chile, in this prospective study we compared the clinical utility of Al[^{18}F]F-NOTA-Octreotide PET/CT imaging with [^{68}Ga]Ga-DOTA-TATE PET/CT and clinical parameters of NET patients in the Latin-American population.

2. Materials and Methods

2.1. Radiochemistry

Al[^{18}F]F-NOTA-Octreotide was produced in accordance with local GMP-regulations using a modified procedure similar to a process previously described [23] and as detailed in the supplemental information (Figures S2–S4, Tables S1 and S2). Briefly, 35 ± 19 GBq (range 8.1–54.6 GBq) Al[^{18}F]F-NOTA-Octreotide were obtained from starting activities of 100 ± 51 GBq (range: 40–170 GBq) as a sterile solution after 31 min in 33.7 ± 8.9% (N = 8) radiochemical yield (n.d.c.), >95% radiochemical purity, and specific activities of 114 ± 61 GBq/μmol. For further details regarding specifications and results, see SI.

2.2. PET/CT Imaging

A total of 20 patients (age: 57.3 ± 11.1 y) with biopsy-proven, stage IV NET and complying with all inclusion criteria (see SI) were enrolled in this prospective study (Table 1). Al[^{18}F]F-NOTA-Octreotide and [^{68}Ga]Ga-DOTA-TATE were injected intravenously at a dose of 222–296 MBq and 148–185 MBq, respectively, and PET/CT images were acquired head-to-mid-thigh at 60 ± 10 min post injection (Biograph Vision, Siemens, Erlangen, Germany). In some cases, we had protocol deviations with lower injected activities (Table 1).

The time interval between both PET/CT scans was 12.7 ± 8.0 days (range: 2–30 days), without any treatment during the interval. A low dose CT and contrast-enhanced CT scan was performed for anatomical localisation and attenuation correction for Al[^{18}F]F-NOTA-Octreotide and [^{68}Ga]Ga-DOTA-TATE PET/CT, respectively.

Table 1. Patients' characteristics.

Patient ID	Age (y)	Gender	Primary Tumour	Tumour Grade	Ki-67 Index	[^{68}Ga]Ga-DOTA-TATE Activity (MBq)	Al[^{18}F]F-NOTA-Octreotide Activity (MBq)	Delay (Days)
1	73	M	Small Intestine	G2	6%	156.1	262.3	7
2	45	F	Bronchial	G1	1%	152.1	185.0	7
3	49	M	Pancreas	G2	8%	126.2	272.7	2
4	44	M	Pancreas	G2	5%	149.5	282.7	2
5	73	M	Apendice cecal	G1	1%	141.3	301.9	23
6	69	M	Small Intestine	G2	5%	165.8	265.3	23
7	60	M	Small Intestine	G1	1%	159.8	276.0	30
8	58	M	Small Intestine	G1	1%	95.8	284.9	23
9	40	M	Small Intestine	G2	12%	179.8	214.6	6
10	42	M	Liver	G3	>20%	143.2	236.8	22
11	57	F	Unknown	G3	30%	146.2	251.6	8
12	57	F	Colon	G2	15%	172.4	254.2	7
13	60	F	Small Intestine	G1	2%	172.1	232.3	7
14	54	F	Small Intestine	G2	NA	97.7	256.8	13
15	63	F	Small Intestine	G2	5%	165.8	163.9	8
16	60	M	Unknown	G2	NA	131.0	237.1	8
17	52	M	Small Intestine	G1	1%	175.0	254.9	13
18	55	M	Small Intestine	G2	5%	145.0	245.6	15
19	83	F	Small Intestine	G2	3%	152.8	252.0	16
20	52	M	Small Intestine	G2	3%	153.5	205.7	15

2.3. Image Analysis

Volumes of interest (VOIs) were drawn around tumour lesions, visually distinguished as regions of increased radiotracer uptake relative to background uptake and expected physiological radiotracer uptake. To perform semi-quantitative analysis, mean, peak and maximum standard uptake values (SUV_{bw}) were calculated using Siemens SyngoVia software. Two nuclear medicine experts who were not blinded to clinical data, independently analysed the PET images. The biodistribution profiles in normal organs were compared for both tracers by analysing SUV_{mean} and SUV_{max} values. Likewise, SUV_{max} and SUV_{peak} values were used to compare the uptake of Al[^{18}F]F-NOTA-Octreotide and [^{68}Ga]Ga-DOTA-TATE in NET lesions. Tumour-to-liver (TLR) and tumour-to-spleen ratios (TSR) were calculated by dividing the SUV_{max} of different tumour lesions by the SUV_{mean} of the liver and spleen, respectively.

2.4. Statistical Analysis

Continuous variables were evaluated for normal distribution with histograms and Q-Q plots. Nonparametric quantitative data were compared using a two-sided Wilcoxon signed-rank test to analyse and compare SUV, TLR, and TSR values between scans with p-values < 0.05 considered as statistically significant. To test the non-inferiority of Al[^{18}F]F-

NOTA-Octreotide compared to [^{68}Ga]Ga-DOTA-TATE, malignant lesions detected in each patient were registered and counted. In the case of an excessive number of lesions (≥50) an arbitrary number of 50 lesions was used. Since cancerous lesions within a subject are likely to be more correlated than cancerous lesions between subjects, a linear mixed-effects model of non-inferiority for repeated measures was employed [24]. The study had a clinically significant non-inferiority margin of 5% to show a non-inferiority of Al[^{18}F]F-NOTA-Octreotide compared to [^{68}Ga]Ga-DOTA-TATE in tumoral lesion detection, with 80% power and an alpha of 2.5% (one-sided). R version 4.2.0 (22 April 2022) was used for all statistical analyses[25].

3. Results

3.1. Biodistribution of [^{68}Ga]Ga-DOTA-TATE Compared to Al[^{18}F]F-NOTA-Octreotide

In this prospective study, 20 patients with biopsy-proven NET were enrolled to compare the biodistribution and clinical utility of [^{68}Ga]Ga-DOTA-TATE and Al[^{18}F]F-NOTA-Octreotide. No adverse events, adverse drug reactions or significant changes in vital signs were observed during the study. Both tracers showed similar physiological uptake in spleen, vascular pool and bone. However, [^{68}Ga] Ga-DOTA-TATE exhibited significantly higher uptake in liver ($p < 0.01$), hypophysis ($p < 0.01$), salivary glands ($p < 0.01$), uncinate process ($p < 0.05$), adrenal glands ($p < 0.01$), kidneys ($p < 0.05$) and small intestine ($p < 0.05$). The highest uptake of Al[^{18}F]F-NOTA-Octreotide was observed in the spleen, adrenal glands and kidneys, whereas a low uptake was observed for vascular pool, salivary glands and bone, a pattern similar to that seen with [^{68}Ga]Ga-DOTA-TATE (Figure 1).

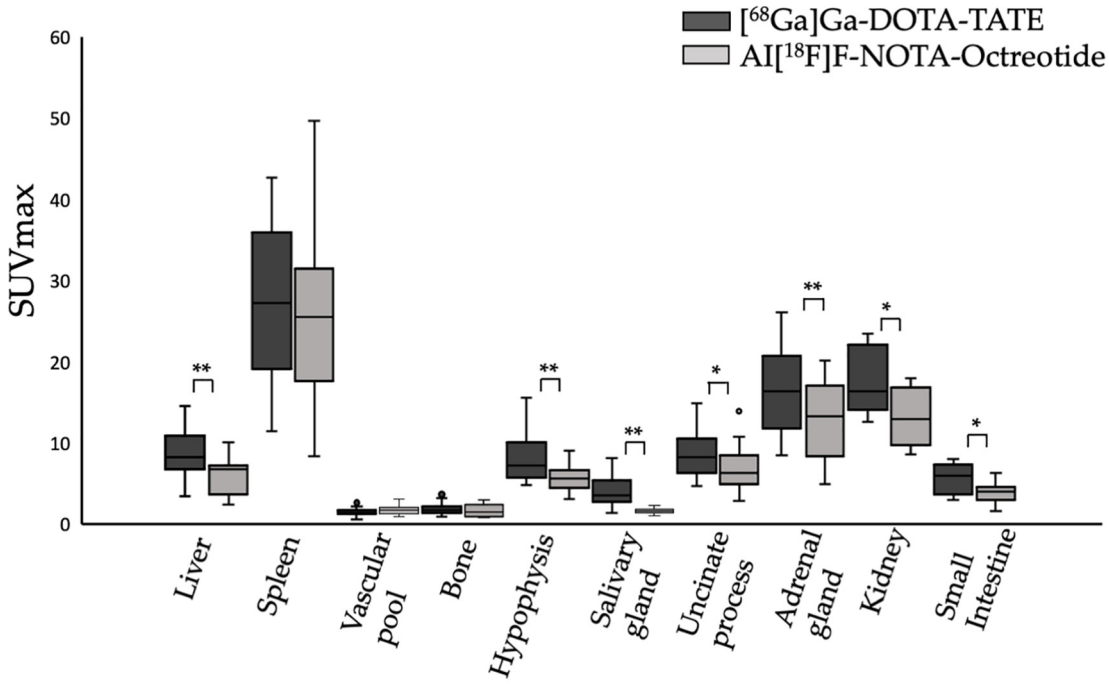

Figure 1. Physiological uptake (SUVmax) of [^{68}Ga]Ga-DOTA-TATE (black bars) and Al[^{18}F]F-NOTA-Octreotide (grey bars) in different tissues. * ($p < 0.05$), ** ($p < 0.001$).

Tumour uptake of [^{68}Ga]Ga-DOTA-TATE and Al[^{18}F]F-NOTA-Octreotide was compared by means of SUV_{max} values and tumour-to-background ratios. [^{68}Ga]Ga-DOTA-TATE showed higher uptake in liver (SUVmax: 8.76 ± 2.84 vs. 6.11 ± 2.24), hypophysis (SUVmax: 8.12 ± 3.05 vs. 5.75 ± 1.68), salivary glands (SUVmax: 4.1 ± 1.83 vs. 1.68 ± 0.29), uncinate process (SUVmax: 8.58 ± 2.91 vs. 6.82 ± 2.73), adrenal glands (SUVmax: 16.42 ± 4.8 vs. 12.75 ± 4.65), kidneys (SUVmax: 17.64 ± 4.01 vs. 13.41 ± 3.63) and small intestine (SUVmax: 5.73 ± 1.78 vs. 3.9 ± 1.33) as compared to Al[^{18}F]F-NOTA-Octreotide. (Figure 1, Table 2).

Table 2. [^{68}Ga]Ga-DOTA-TATE PET and Al[^{18}F]F-NOTA-Octreotide PET SUV_{max} values.

Organ	[^{68}Ga]Ga-DOTA-TATE SUV_{max}	Al[^{18}F]F-NOTA-Octreotide SUV_{max}	*p*-Value
Liver	8.76 ± 2.83	6.11 ± 2.23	<0.001
Spleen	27.18 ± 9.91	25 ± 10.91	0.247
Vascular pool	1.543 ± 0.62	1.71 ± 0.54	0.07
Bone	1.86 ± 0.68	1.66 ± 0.74	0.262
Hypophysis	8.11 ± 3.05	5.75 ± 1.68	<0.001
Salivary gland	4.1 ± 1.83	1.61 ± 0.29	<0.001
Uncinate process	8.58 ± 2.91	6.82 ± 2.73	<0.05
Adrenal gland	16.42 ± 4.8	12.75 ± 4.65	<0.001
Kidney	17.64 ± 4	13.4 ± 3.63	<0.05
Small intestine	5.73 ± 1.88	3.9 ± 1.33	<0.05

[^{68}Ga]Ga-DOTA-TATE showed higher tumour-to-liver ratios in lymph nodes metastasis (TLR: 3.8 ± 3.9 vs. 3.3 ± 2.3) and distant metastasis in lung, ovary, soft tissue and peritoneal carcinomatosis (TLR: 3.6 ± 6.0 vs. 3.1 ± 3.7) as compared to Al[^{18}F]F-NOTA-Octreotide. On the contrary, metastatic lesions showed higher tumour-to-background ratios with Al[^{18}F]F-NOTA-Octreotide in bone(TLR: 3.0 ± 1.8 vs. 2.1 ± 0.8) and primary tumour (TLR: 6.0 ± 2.9 vs. 4.8 ± 2.4, respectively) than with [^{68}Ga]Ga-DOTA-TATE. We obtained similar results when calculating tumour-to-background ratios with spleen as reference organ. However, differences in TLR and TSR values were not statistically significant (Figure 2).

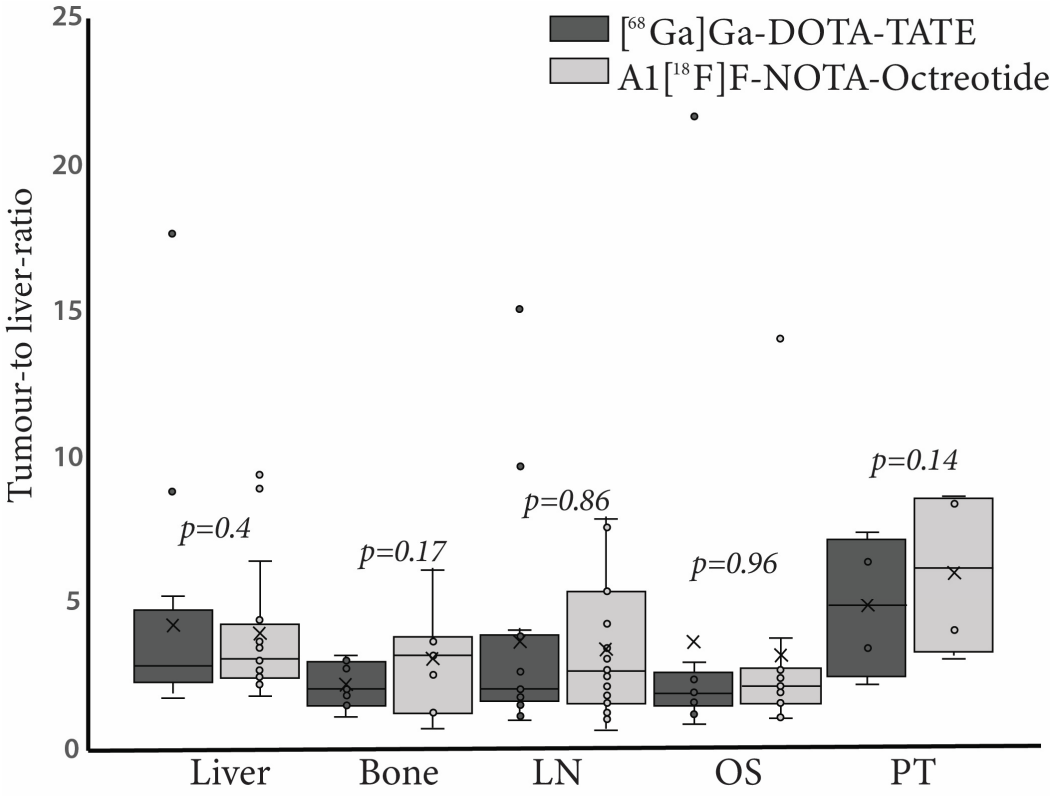

Figure 2. Tumour-to-liver ratio (TLR) of [^{68}Ga]Ga-DOTA-TATE (black bars) and Al[^{18}F]F-NOTA-Octreotide (grey bars) in different tissues. Right panel, boxplots representing TLR in liver, bone, lymph node (LN), other sites (OS) and primary tumour (PT). In each case outliers are represented as circles.

3.2. Tumoral Lesion Detection of [^{68}Ga]Ga-DOTA-TATE Compared to Al[^{18}F]F-NOTA-Octreotide

Next, we compared the number of lesions detected by [^{68}Ga]Ga-DOTA-TATE and Al[^{18}F]F-NOTA-Octreotide. Only four patients showed malignant lesions in the primary tumour site. For these patients, both tracers revealed the exact number of malignant lesions. While both tracers revealed liver metastasis in the same patients (17/20 patients), [^{68}Ga]Ga-DOTA-TATE detected one additional metastatic lesion in patients No. 2, No. 14 and No. 15 and two additional lesions in patient No. 19 as compared to Al[^{18}F]F-NOTA-Octreotide (Figure S5). In contrast, patient No. 10, showed one additional metastatic lesion with Al[^{18}F]F-NOTA-Octreotide compared to [^{68}Ga]Ga-DOTA-TATE (Figure 3). Despite these differences, all patients exhibited numerous metastatic lesions (Table 3) with a positive [^{68}Ga]Ga-DOTA-TATE PET scan in total 366 metastatic lesions in the liver and Al[^{18}F]F-NOTA-Octreotide PET detecting 362 lesions.

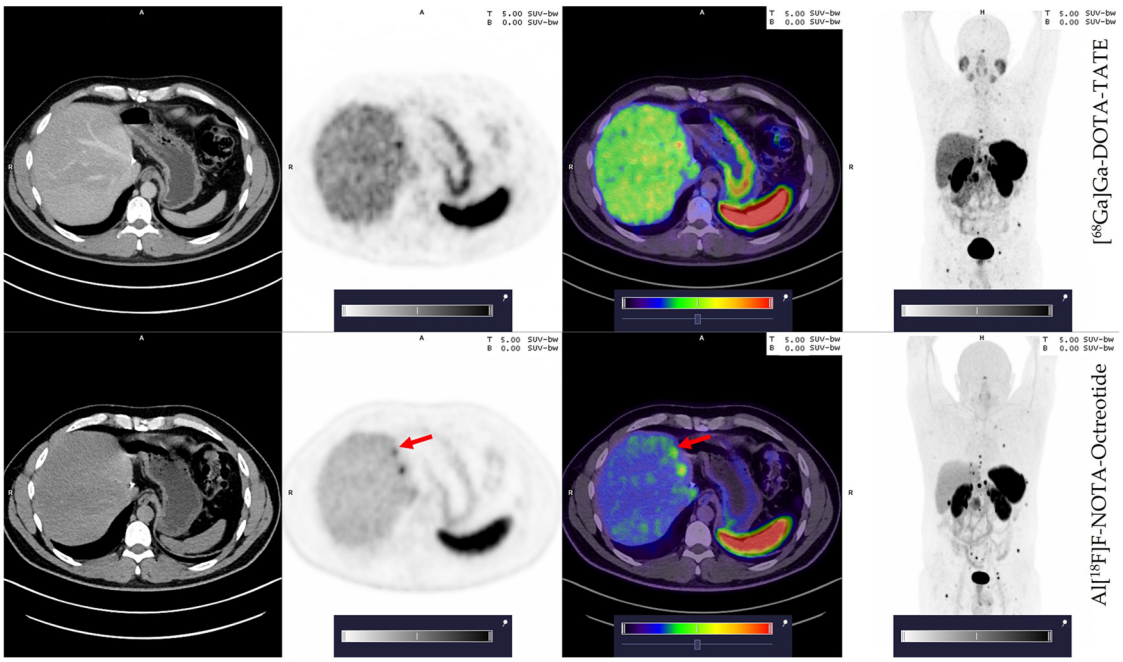

Figure 3. Patient 10; 42 years old, male with an additional small liver lesion (red arrow) detected by Al[^{18}F]F-NOTA-Octreotide (lower row) and not seen with [^{68}Ga]Ga-DOTA-TATE (upper row). Colour scale bar representing SUV values ranging from 0.0–5.0.

Table 3. Neoplastic lesions detected with [^{68}Ga]Ga-DOTA-TATE and Al[^{18}F]F-NOTA-Octreotide.

Patients	**Primary Tumour**		**Liver Metastases ****		**Bone Metastases**		**LN Metastases**		**Other Sites Metastases**		**Total Lesions**	
Tracer *	GAD	FOC	GAD	FOC	GAD	FOC	GAD	FOC	GAD	FOC	GAD	FOC
1	0	0	1	1	15	15	10	10	0	0	26	26
2	1	1	**10**	**9**	6	6	1	1	0	0	18	17
3	1	1	10	10	0	0	0	0	0	0	11	11
4	1	1	5	5	0	0	0	0	0	0	6	6
5	0	0	27	27	3	3	25	25	1	1	≥50	≥50
6	1	1	0	0	0	0	11	11	1	1	13	13
7	0	0	≥50	≥50	0	0	3	3	0	0	≥50	≥50

Table 3. *Cont.*

Patients	Primary Tumour		Liver Metastases **		Bone Metastases		LN Metastases		Other Sites Metastases		Total Lesions	
8	0	0	2	2	0	0	4	4	1	1	7	7
9	0	0	0	0	0	0	4	4	0	0	4	4
10	0	0	**2**	**3**	16	16	2	2	3	3	23	24
11	0	0	≥50	≥50	≥50	≥50	0	0	0	0	≥50	≥50
12	0	0	8	8	0	0	0	0	3	3	11	11
13	0	0	>50	>50	≥50	≥50	13	13	2	2	≥50	≥50
14	0	0	**20**	**19**	0	0	1	1	3	3	24	23
15	0	0	**16**	**15**	0	0	1	1	1	1	18	17
16	0	0	0	0	11	11	4	4	2	2	17	17
17	0	0	2	2	0	0	1	1	0	0	3	3
18	0	0	≥50	≥50	0	0	31	31	≥50	≥50	≥50	≥50
19	0	0	**13**	**11**	1	1	1	1	≥50	≥50	≥50	≥50
20	0	0	≥50	≥50	0	0	0	0	0	0	≥50	≥50

* GAD: [^{68}Ga]Ga-DOTA-TATE; FOC: Al[^{18}F]F-NOTA-Octreotide. ** Patients with discordant lesions are highlighted in bold. Patients where [^{68}Ga]Ga-DOTA-TATE detected more lesions are highlighted in blue, where Al[^{18}F]F-NOTA-Octreotide detected more lesions are highlighted in yellow.

Hence, to determine a non-inferior detection of neoplastic lesions of Al[^{18}F]F-NOTA-Octreotide PET compared to [^{68}Ga]Ga-DOTA-TATE PET we employed a multilevel model since the results indicated evidence of clustering, confirmed by the correlation coefficient (0.68) and with a significant ANOVA test ($p < 0.05$). The results showed a mean difference, test-reference, of 0.074% (95% confidence interval: −3.874–4.022%) with a lower margin higher than the pre-specified boundary for non-inferiority (-5%), indicating that Al[^{18}F]F-NOTA-Octreotide PET is non-inferior to [^{68}Ga]Ga-DOTA-TATE PET (Figure 4).

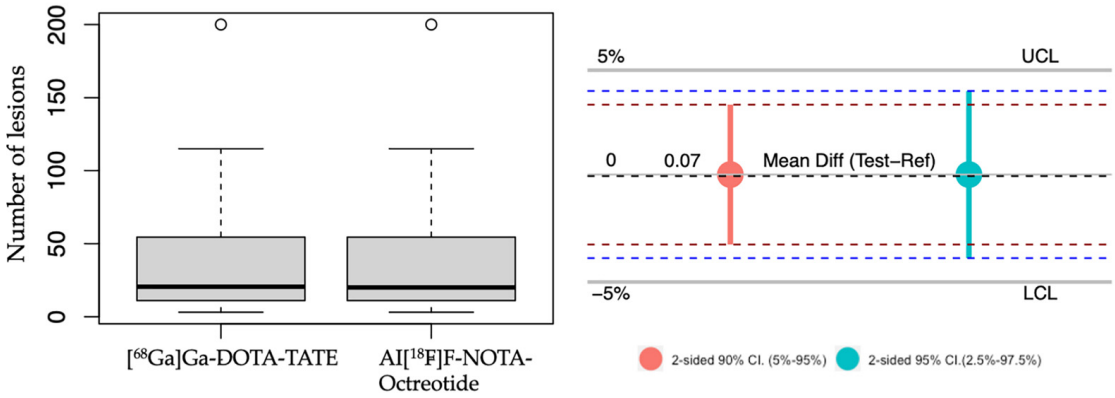

Figure 4. Non-inferiority analysis. Left panel, boxplot representing the average of tumoral lesions detected with [^{68}Ga]Ga-DOTA-TATE and Al[^{18}F]F-NOTA-Octreotide. right panel, a non-inferiority chart 2-sided 90% confidence interval (red) and 95% confidence interval (light blue). UCL: upper clinically significant margin limit 5%. LCL: lower clinically significant margin limit of 5%. The mean difference is indicated. Outliers are represented as circles.

4. Discussion

^{68}Ga-labelled tracers for SSTR are the gold standard for imaging NET patients. However, countries with vast territorial areas and limited ^{68}Ge/^{68}Ga generators face an enormous logistical challenge. Al[^{18}F]F-NOTA-Octreotide has emerged as an exciting alternative to ^{68}Ga-tracers, especially due to the longer half-life of fluorine-18 compared to gallium-68 and production yield, facilitating distribution to distant clinical facilities. Moreover, fluorine-18 presents a shorter positron range resulting in an improved spatial resolution compared to gallium-68 [17].

To evaluate Al[^{18}F]F-NOTA-Octreotide clinical utility, we performed a prospective study on 20 patients to compare [^{68}Ga]Ga-DOTA-TATE versus Al[^{18}F]F-NOTA-Octreotide. The biodistribution profile of Al[^{18}F]F-NOTA-Octreotide and [^{68}Ga]Ga-DOTA-TATE was comparable for the spleen showing high uptake with SUV_{max} values of 25.0 and 27.2, respectively. However, Al[^{18}F]F-NOTA-Octreotide showed significantly less accumulation in the liver, hypophysis, salivary glands, uncinate process, adrenal gland, kidney, and small intestine compared to [^{68}Ga]Ga-DOTA-TATE. The differences in uptake were most pronounced in salivary glands which is in line with previous studies reporting four to sixfold higher uptake [21]. Collectively our results revealed a high background uptake for [^{68}Ga]Ga-DOTA-TATE compared to Al[^{18}F]F-NOTA-Octreotide, which is consistent with previously published data [14]. However, while writing the present article, a new multicentric prospective study including a cohort of 75 NET patients histologically confirmed was published showing no significant differences in mean SUV_{max} in most organs [22]. Contrary to this report, we observed a higher mean SUV_{max} for [^{68}Ga]Ga-DOTA-TATE compared to Al[^{18}F]F-NOTA-Octreotide. This discrepancy may be due to the smaller group sample included in our study (20 patients). When the mean of the tumour-to-background ratio was analysed (using the liver, TLR, and spleen, TSR, as background tissue), non-significant differences were observed (Fig 2), demonstrating a lower liver and spleen background with Al[^{18}F]F-NOTA-Octreotide compared to [^{68}Ga]Ga-DOTA-TATE.

Previous studies have shown that both [^{68}Ga]Ga-DOTA-TATE and Al[^{18}F]F-NOTA-Octreotide are highly sensitive to detecting NET lesions. In fact, Hou et al., (2021) showed in a group of 20 patients that Al[^{18}F]F-NOTA-Octreotide detected 177 lesions compared to 152 lesions with [^{68}Ga]Ga-DOTA-TATE. This difference was particularly observed in the liver (116 vs. 93). Likewise, Pauwels, et al., 2022 showed that the detection ratio means of Al[^{18}F]F-NOTA-Octreotide was significantly higher compared to [^{68}Ga]Ga-DOTA-TATE/NOC (91.1% vs. 75.3% lesions). The differential detection ratio (calculated by the difference in detection ratio between Al[^{18}F]F-NOTA-Octreotide and [^{68}Ga]Ga-DOTA-TATE/NOC per each patient) was used to evaluate whether Al[^{18}F]F-NOTA-Octreotide was non-inferior to [^{68}Ga]Ga-DOTA-TATE and [^{68}Ga]Ga-DOTA-NOC. This study concluded that Al[^{18}F]F-NOTA-Octreotide was non-inferior compared to [^{68}Ga]Ga-DOTA-TATE/NOC PET in NET patients [22].

Our study included patients with NETs (mainly G1/G2), which, in some cases, obstructed the lesions counting process. Thus, patients No. 7, No. 11, 13, 18, and 20 presented countless liver metastasis, which was registered as $\geq$50 lesions. This was also true for bone metastasis in the case of patients 11 and 13 (Table 2). In total, 748 lesions were detected (considering countless metastasis as at least 50 lesions), 751 with [^{68}Ga]Ga-DOTA-TATE and 747 with Al[^{18}F]F-NOTA-Octreotide.

In the liver, patients No. 2 [^{68}Ga]Ga-DOTA-TATE detected 10 lesions compared to 9 detected by Al[^{18}F]F-NOTA-Octreotide. Likewise, in the patient N°14 [^{68}Ga]Ga-DOTA-TATE detected 20 lesions compared to 19 detected by Al[^{18}F]F-NOTA-Octreotide, and in the patient No. 15 [^{68}Ga]Ga-DOTA-TATE detected 16 lesions and Al[^{18}F]F-NOTA-Octreotide only 15. In the case of patient No. 19, [^{68}Ga]Ga-DOTA-TATE detected two more lesions compared to Al[^{18}F]F-NOTA-Octreotide (13 vs. 11, respectively). In the case of patient No. 10, Al[^{18}F]F-NOTA-Octreotide detected one more lesion than [^{68}Ga]Ga-DOTA-TATE (3 vs. 2, respectively) (Figure 3). Interestingly, this patient presented a G3 NET tumour. This particular lesion was small, suggesting that ^{18}F presents a superior capacity than [^{68}Ga]Ga-DOTA-TATE to detect small lesions. This hypothesis is supported by the better spatial resolution of fluorine-18 compared to gallium-68 and by previous results with comparison using both tracers to detect < 5mm peritoneal metastasis [14,26].

The differences between both tracers in detecting liver lesions neither change the therapeutic approach nor the disease prognosis. In fact, none of these differences was statistically significant. In other metastatic lesions such as primary tumour, bone, lymph nodes, soft tissue, ovary lung or peritoneal carcinomatosis, [^{68}Ga]Ga-DOTA-TATE and Al[^{18}F]F-NOTA-Octreotide had comparable effectiveness, detecting the same number of lesions.

Our results confirm that Al[^{18}F]F-NOTA-Octreotide is not inferior to [^{68}Ga]Ga-DOTA-TATE PET to detect lesions in NET patients since the lower margin of the 95% of the confidence interval was higher than the lower pre-specified boundary of −5% for non-inferiority (Figure 4). Thus, our results confirmed previous results [14,22] in Latin-American NET patients in which the distribution and production of radiotracers is a crucial challenge, especially considering the geography and prevalence of cancer [27].

Our study found non-significant differences in detection rates between Al[^{18}F]F-NOTA-Octreotide and [^{68}Ga]Ga-DOTA-TATE PET. However, one limitation of our study is the small subgroup of patients included and missing complementary data such as other imaging modalities, such as magnetic resonance imaging or ^{18}F-FDG PET/CT imaging. Ongoing research at our centre is now focused on evaluating the relationship between the tumoral grade and lesion uptake in larger groups of patients.

5. Conclusions

Our study is the first, to our knowledge, to be performed on Latin-American NET patients. Our results show that Al[^{18}F]F-NOTA-Octreotide exhibits a similar biodistribution to that of [^{68}Ga]Ga-DOTA-TATE, with similar detection rates in different organs, demonstrating the non-inferiority of Al[^{18}F]F-NOTA-Octreotide-PET/CT compared to [^{68}Ga]Ga-DOTA-TATE-PET/CT. Therefore, Al[^{18}F]F-NOTA-Octreotide is an important alternative for NET patients, especially in countries (such as Chile) with vast territories and limited ^{68}Ge/^{68}Ga generators. Future studies should include more patients to evaluate the clinical utility of Al[^{18}F]F-NOTA-Octreotide for staging NET cancer patients and evaluate the potential detection of small and less differentiated lesions.

Supplementary Materials: The following supporting information can be downloaded at: https://www.mdpi.com/article/10.3390/cancers15020439/s1, Figure S1: Chemical structures of DOTA-TATE and NOTA-Octreotide with differences highlighted in colored areas; Figure S2: Synthera®+ Synthesizer with loaded IFP and reagents (left), IFP with reagents and cartridges; Figure S3: Representative HPLC-Chromatogram for Al[^{18}F]F-NOTA-Octreotide; UV signal (upper row) and radioactivity (lower row). Product elutes at 12.4 min (isomer 1) and 13.0 min (isomer 2) and main impurity is [^{18}F]F- eluting at 1.2 min. The UV peak at t = 0.8 corresponds to ascorbate; Figure S4: Zoom of HPLC-Chromatogram in figure S2. for Al[^{18}F]F-NOTA-Octreotide; UV signal (upper row) and radioactivity (lower row). Product elutes at 12.4 min (isomer 1) and 13.0 min (isomer 2) and main impurity is [^{18}F]F- eluting at 1.2 min. The UV peak at t = 0.8 corresponds to ascorbate; Figure S5: (A) Patient ID 2, (45 y, female) with a dominant right liver lesion (red arrow) with significantly higher uptake with [^{68}Ga]Ga-DOTA-TATE (upper row) versus Al[^{18}F]F-NOTA-Octreotide (lower row). Color scale bars representing SUV values ranging from 0.0–5.0.; Table S1: Representative batches (last 5 executed) for the production of Al[18F]F-NOTA-Octreotide; Table S2: Release specifications and overall QC results for Al[^{18}F]F-NOTA-octreotide—There is no US Pharmacopoeia monograph available. Where applicable, the specifications have been based on the existing USP for [^{68}Ga]Ga-DOTA-TATE.

Author Contributions: Study design and conceptualization, V.K., R.F. and H.A.; radiochemistry, V.K., E.E. and N.E.; data collection, image acquisition and reconstruction, A.H.d.M. and J.W.; formal analysis, A.H. and R.F.; data interpretation and statistical analysis, A.H. and C.S.-R.; original manuscript preparation, C.S.-R.; review and editing, all; supervision, R.F. All authors have read and agreed to the published version of the manuscript.

Funding: This research received non-financial support from Ion Beam Applications, Louvain-la-Neuve, Belgium. No further external funding was received.

Institutional Review Board Statement: All procedures performed in studies involving human participants were in accordance with the ethical standards of the institutional and national research committee and with the principles of the 1964 Declaration of Helsinki and its later amendments or comparable ethical standards. The study was approved by the regional ethics committee board (CEC SSM Oriente, permit number 11082020) and written informed consent has been obtained from all participants.

Informed Consent Statement: Informed consent was obtained from all subjects involved in the study.

Data Availability Statement: The data presented in this study are available on request from the corresponding author. The data are not publicly available due to restrictions regarding privacy of patients and ethical reasons.

Acknowledgments: We would like to thank Maria Jesus Yaryes, Jorge Perez and Matias Ceballos (all Positronmed) for their help during PET studies and data acquisition. We are also grateful for the support of Marcelo Ilheu, Lorena Cantuarias (Positronpharma), Cristiana Gameiro, Benoit Nactergal, David Goblet, and Guillaume Decoux for their assistance in tracer production, method development and validation.

Conflicts of Interest: The authors declare to have no conflict of interest.

References

1. Barakat, M.T.; Meeran, K.; Bloom, S.R. Neuroendocrine tumours. *Endocr. Relat. Cancer* **2004**, *11*, 1–18. [CrossRef]
2. Yao, J.C.; Hassan, M.; Phan, A.; Dagohoy, C.; Leary, C.; Mares, J.E.; Abdalla, E.K.; Fleming, J.B.; Vauthey, J.N.; Rashid, A.; et al. One hundred years after "carcinoid": Epidemiology of and prognostic factors for neuroendocrine tumors in 35,825 cases in the United States. *J. Clin. Oncol.* **2008**, *26*, 3063–3072. [CrossRef] [PubMed]
3. Modlin, I.M.; Oberg, K.; Chung, D.C.; Jensen, R.T.; de Herder, W.W.; Thakker, R.V.; Caplin, M.; Delle Fave, G.; Kaltsas, G.A.; Krenning, E.P.; et al. Gastroenteropancreatic neuroendocrine tumours. *Lancet Oncol.* **2008**, *9*, 61–72. [CrossRef] [PubMed]
4. Hallet, J.; Law, C.H.; Cukier, M.; Saskin, R.; Liu, N.; Singh, S. Exploring the rising incidence of neuroendocrine tumors: A population-based analysis of epidemiology, metastatic presentation, and outcomes. *Cancer* **2015**, *121*, 589–597. [CrossRef]
5. Sackstein, P.E.; O'Neil, D.S.; Neugut, A.I.; Chabot, J.; Fojo, T. Epidemiologic trends in neuroendocrine tumors: An examination of incidence rates and survival of specific patient subgroups over the past 20 years. *Semin. Oncol.* **2018**, *45*, 249–258. [CrossRef] [PubMed]
6. Mittra, E.S. Neuroendocrine Tumor Therapy: (177)Lu-DOTATATE. *AJR Am. J. Roentgenol.* **2018**, *211*, 278–285. [CrossRef]
7. Tomita, T. Significance of chromogranin A and synaptophysin in pancreatic neuroendocrine tumors. *Bosn. J. Basic Med. Sci.* **2020**, *20*, 336–346. [CrossRef]
8. Hofland, L.J.; Lamberts, S.W.; van Hagen, P.M.; Reubi, J.C.; Schaeffer, J.; Waaijers, M.; van Koetsveld, P.M.; Srinivasan, A.; Krenning, E.P.; Breeman, W.A. Crucial role for somatostatin receptor subtype 2 in determining the uptake of [111In-DTPA-D-Phe1]octreotide in somatostatin receptor-positive organs. *J. Nucl. Med.* **2003**, *44*, 1315–1321.
9. Banerjee, S.R.; Pomper, M.G. Clinical applications of Gallium-68. *Appl. Radiat. Isot.* **2013**, *76*, 2–13. [CrossRef]
10. Poeppel, T.D.; Binse, I.; Petersenn, S.; Lahner, H.; Schott, M.; Antoch, G.; Brandau, W.; Bockisch, A.; Boy, C. 68Ga-DOTATOC versus 68Ga-DOTATATE PET/CT in functional imaging of neuroendocrine tumors. *J. Nucl. Med.* **2011**, *52*, 1864–1870. [CrossRef]
11. Bozkurt, M.F.; Virgolini, I.; Balogova, S.; Beheshti, M.; Rubello, D.; Decristoforo, C.; Ambrosini, V.; Kjaer, A.; Delgado-Bolton, R.; Kunikowska, J.; et al. Guideline for PET/CT imaging of neuroendocrine neoplasms with (68)Ga-DOTA-conjugated somatostatin receptor targeting peptides and (18)F-DOPA. *Eur. J. Nucl. Med. Mol. Imaging* **2017**, *44*, 1588–1601. [CrossRef]
12. Hope, T.A.; Bergsland, E.K.; Bozkurt, M.F.; Graham, M.; Heaney, A.P.; Herrmann, K.; Howe, J.R.; Kulke, M.H.; Kunz, P.L.; Mailman, J.; et al. Appropriate Use Criteria for Somatostatin Receptor PET Imaging in Neuroendocrine Tumors. *J. Nucl. Med.* **2018**, *59*, 66–74. [CrossRef] [PubMed]
13. Amaral, H.; Pruzzo, R.; Fernández, R.; Kramer, V.; Soza-Ried, C.; Coudeu, I. Chilean experience using "Theranostics" for treating metastatic neuroendocrine tumors with [177Lu]Lu DOTA-TATE. *Arch. Clin. Gastroenterol.* **2020**, *6*, 5.
14. Hou, J.; Long, T.; He, Z.; Zhou, M.; Yang, N.; Chen, D.; Zeng, S.; Hu, S. Evaluation of (18)F-AlF-NOTA-octreotide for imaging neuroendocrine neoplasms: Comparison with (68)Ga-DOTATATE PET/CT. *EJNMMI Res.* **2021**, *11*, 55. [CrossRef]
15. Long, T.; Yang, N.; Zhou, M.; Chen, D.; Li, Y.; Li, J.; Tang, Y.; Liu, Z.; Li, Z.; Hu, S. Clinical Application of 18F-AlF-NOTA-Octreotide PET/CT in Combination With 18F-FDG PET/CT for Imaging Neuroendocrine Neoplasms. *Clin. Nucl. Med.* **2019**, *44*, 452–458. [CrossRef] [PubMed]
16. Waldmann, C.M.; Stuparu, A.D.; van Dam, R.M.; Slavik, R. The Search for an Alternative to [(68)Ga]Ga-DOTA-TATE in Neuroendocrine Tumor Theranostics: Current State of (18)F-labeled Somatostatin Analog Development. *Theranostics* **2019**, *9*, 1336–1347. [CrossRef] [PubMed]
17. Laverman, P.; McBride, W.J.; Sharkey, R.M.; Eek, A.; Joosten, L.; Oyen, W.J.; Goldenberg, D.M.; Boerman, O.C. A novel facile method of labeling octreotide with (18)F-fluorine. *J. Nucl. Med.* **2010**, *51*, 454–461. [CrossRef]
18. Laverman, P.; D'Souza, C.A.; Eek, A.; McBride, W.J.; Sharkey, R.M.; Oyen, W.J.; Goldenberg, D.M.; Boerman, O.C. Optimized labeling of NOTA-conjugated octreotide with F-18. *Tumor Biol.* **2012**, *33*, 427–434. [CrossRef]
19. Leyton, J.; Iddon, L.; Perumal, M.; Indrevoll, B.; Glaser, M.; Robins, E.; George, A.J.; Cuthbertson, A.; Luthra, S.K.; Aboagye, E.O. Targeting somatostatin receptors: Preclinical evaluation of novel 18F-fluoroethyltriazole-Tyr3-octreotate analogs for PET. *J. Nucl. Med.* **2011**, *52*, 1441–1448. [CrossRef]
20. Pauwels, E.; Cleeren, F.; Tshibangu, T.; Koole, M.; Serdons, K.; Dekervel, J.; Van Cutsem, E.; Verslype, C.; Van Laere, K.; Bormans, G.; et al. Al(18)F-NOTA-octreotide: First comparison with (68)Ga-DOTATATE in a neuroendocrine tumour patient. *Eur. J. Nucl. Med. Mol. Imaging* **2019**, *46*, 2398–2399. [CrossRef]

21. Pauwels, E.; Cleeren, F.; Tshibangu, T.; Koole, M.; Serdons, K.; Dekervel, J.; Van Cutsem, E.; Verslype, C.; Van Laere, K.; Bormans, G.; et al. [(18)F]AlF-NOTA-octreotide PET imaging: Biodistribution, dosimetry and first comparison with [(68)Ga]Ga-DOTATATE in neuroendocrine tumour patients. *Eur. J. Nucl. Med. Mol. Imaging* **2020**, *47*, 3033–3046. [CrossRef] [PubMed]
22. Pauwels, E.; Cleeren, F.; Tshibangu, T.; Koole, M.; Serdons, K.; Boeckxstaens, L.; Dekervel, J.; Vandamme, T.; Lybaert, W.; Van den Broeck, B.; et al. (18)F-AlF-NOTA-octreotide outperforms (68)Ga-DOTA-TATE/-NOC PET in neuroendocrine tumor patients: Results from a prospective, multicenter study. *J. Nucl. Med.* **2022**, *64*. [CrossRef]
23. Tshibangu, T.; Cawthorne, C.; Serdons, K.; Pauwels, E.; Gsell, W.; Bormans, G.; Deroose, C.M.; Cleeren, F. Automated GMP compliant production of [(18)F]AlF-NOTA-octreotide. *EJNMMI Radiopharm. Chem.* **2020**, *5*, 4. [CrossRef] [PubMed]
24. Mascha, E.J. Equivalence and noninferiority testing in anesthesiology research. *Anesthesiology* **2010**, *113*, 779–781. [CrossRef] [PubMed]
25. R Core Team. *R: A Language and Environment for Statistical Computing*; R Foundation for Statistical Computing: Vienna, Austria, 2013. Available online: https://www.R-project.org/ (accessed on 10 August 2022).
26. Conti, M.; Eriksson, L. Physics of pure and non-pure positron emitters for PET: A review and a discussion. *EJNMMI Phys.* **2016**, *3*, 8. [CrossRef] [PubMed]
27. Goss, P.E.; Lee, B.L.; Badovinac-Crnjevic, T.; Strasser-Weippl, K.; Chavarri-Guerra, Y.; St Louis, J.; Villarreal-Garza, C.; Unger-Saldana, K.; Ferreyra, M.; Debiasi, M.; et al. Planning cancer control in Latin America and the Caribbean. *Lancet Oncol.* **2013**, *14*, 391–436. [CrossRef]